Dynamic Modeling and Experimental Validation of a Haptic Finger Based on a McKibben Muscle

Dynamic modeling and experimental validation of a haptic finger based on a McKibben muscle

Walter Franco[1], Daniela Maffiodo, Carlo De Benedictis, Carlo Ferraresi,

Department of Mechanical and Aerospace Engineering, Politecnico di Torino, 10129, Torino, Italy

[1]walter.franco@polito.it

Abstract The paper deals with the implementation of a McKibben pneumatic muscle in a tele-operation robotic system provided with haptic feedback, aimed to the generation of the perception force at the operator's fingertip. The architecture of the device is presented and a dynamic model of the system is proposed. A prototype of the device has been tested in dynamic conditions, and the outcomes have been compared with the numerical results, highlighting that the use of a pneumatic muscle is suitable for the actuation of a haptic finger device.

Keywords: Pneumatic artificial muscle, McKibben muscle, Haptics, Teleoperation, Force reflection, Hand exoskeleton, Human-machine interaction

1. Introduction

Teleoperation deals with the remote control of a device (slave). The teleoperation interface (master) is called *haptic* if able to transmit a force feedback to the operator's hand. In this case, the perception force must be generated by controlled actuators, whose mechanical impedance is relevant to allow the correct human-machine interaction.

Due to their intrinsic self-adaptability to the compliance of the biological tissues, non-conventional deformable actuators, as shape memory alloy actuators [1] or pneumatic deformable actuators [2], may be employed for this purpose. Among the latter, the McKibben pneumatic artificial muscle has been integrated in several haptic manipulators and gloves [3-6].

The aim of this work is to study the feasibility of a haptic device whose architecture is based on a single degree-of-freedom mechanism driven by a McKibben muscle actuator. In the paper, the structure of the device is outlined, and a dynamic mathematical model of the system is described. The performance of the real system has been tested in a virtual environment, evaluating the force exerted on

the operator's finger during a manipulation task. Then, the results of the simulation have been compared to the experimental data in order to validate the model.

2. The device

The device, whose scheme is shown in Figure 1, consists of: a four-bar linkage able to generate a desired path of the index fingertip support; a rotary encoder (Baumer electric, BDK series), used to measure the rotation of one of the links, so as to perform the forward kinematic analysis of the mechanism and calculate the position of the fingertip; a planar beam force sensor (FUTEK Advanced Sensor Technology, Inc., FR1020, maximum load 89N) for the measurement of the force applied to the fingertip, providing the required feedback signal to the perception force control loop; a control unit, that, considering the geometrical and mechanical characteristic of the selected virtual object, generates the force reference signal and the command for the actuator; an actuation system, composed by a McKibben pneumatic muscle (Shadow Robot Company Ltd., London), preloaded with a parallel spring (SPEC® T41660) and supplied by a pressure control proportional valve (FESTO® MPPE-3-1/4-10-010B), driving the coupler of the four-bar mechanism through the application of a tensile force to a polyethylene fiber tendon. The device architecture has been detailed in [7]. The control logic has been developed in MATLAB-Simulink® and implemented by means of dSpace® boards and a user interface designed in ControlDesk®.

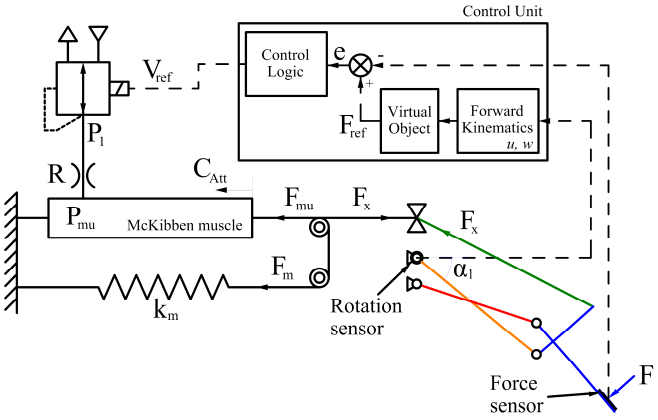

Fig. 1. Scheme of the haptic device.

In Figure 2 the prototype of the device is depicted. The operator rests his hand on the fixed frame of the device, while his fingertip is held by a specially designed support integral with the force sensor mounted on the coupler of the four-bar mechanism.

The operator moves the finger between the position of maximum extension and that of maximum flexion to perform the tele-manipulation of the remote device, and therefore imposes the rotation α_1 of the rocker, measured by the encoder.

Through the forward kinematics evaluation of the mechanism, the control unit calculates the position of the finger in the sagittal plane (u, w) and then, by definition of the shape and the mechanical characteristic of the virtual object, generates the reference force signal F_{ref}. The control unit calculates the error e between the force reference F_{ref} and the measured force F, and provides the command signal for the pressure control proportional valve V_{ref}, used to regulate the upstream pressure of the fluidic resistance p_1. Therefore, the muscle is supplied and consequently pulls the tendon that actuates the coupler of the four-bar mechanism.

As described in [8], the synthesis of the four-bar mechanism was carried out by ensuring that the trajectory of the point P (fingertip holder) should be included into the natural workspace of a finger, calculated by taking into account the dependency among the rotations of each joint (Figure 3a). The lengths of the proximal, middle and distal phalanxes selected are respectively 4 cm, 2.5 cm and 2 cm, while the rotation of the DIP joint has been considered equal to 2/3 of the PIP joint rotation.

The dimensions of the four-bar linkage (Figure 3b) are reported in Table 1. The operator's fingertip is positioned at point P, while the MCP joint is coincident with the fixed hinge O. The tendon 5 is connected to the coupler 2 in X_1, passes through the low-friction support point X, and is pulled by the McKibben muscle.

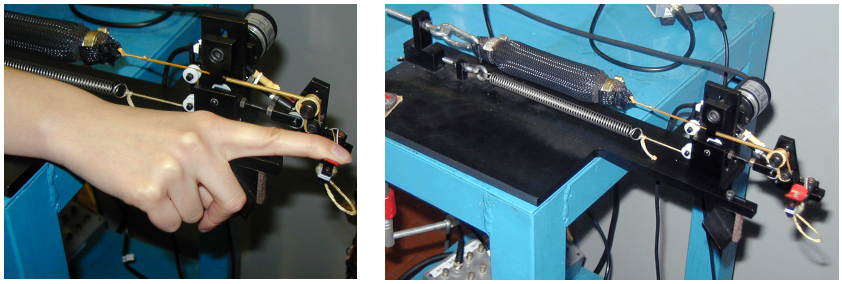

Fig. 2. The prototype of the device.

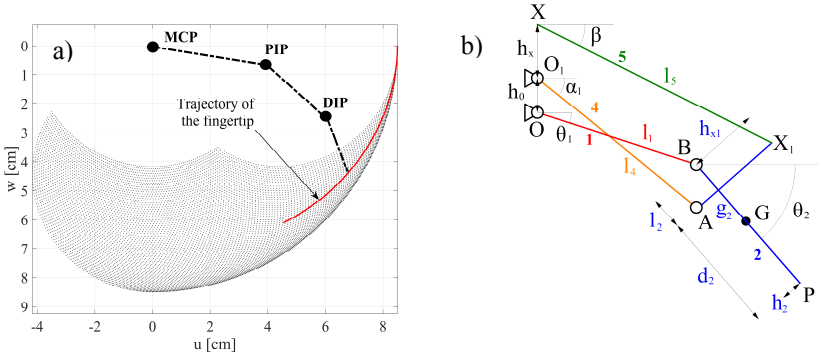

Fig. 3. a): workspace of a human index finger. b): sketch of the mechanism (metacarpophalangeal joint, MCP, proximal inter-phalangeal joint, PIP, and distal inter-phalangeal joint, DIP).

3. The dynamic mathematical model

The block diagram of the dynamic model of the device is presented in Figure 4:

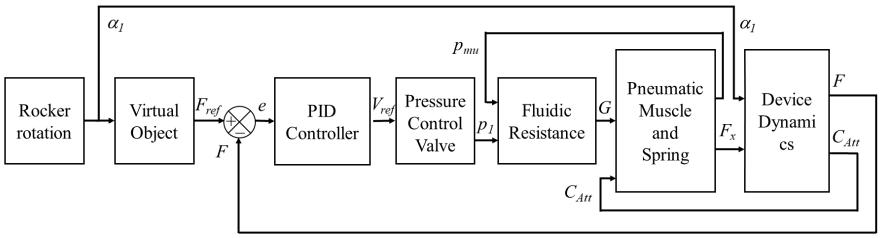

Fig. 4. Block diagram of the device model.

The *Device Dynamics* block calculates the feedback force F applied to the fingertip and the stroke of the McKibben muscle C_{Att}, starting from the rotation of the rocker α_1, imposed by the operator, and the force F_x generated by the combination of the pneumatic muscle and the spring.

The positioning in the sagittal plane (u,w) of each link of the mechanism can be calculated solving the non-linear system of Eq. (1-3):

$$l_4 \cos\alpha_1 + h_2 \sin\vartheta_2 - l_2 \cos\vartheta_2 = l_1 \cos\vartheta_1 \tag{1}$$

$$l_4 \sin\alpha_1 - h_2 \cos\vartheta_2 - l_2 \sin\vartheta_2 - h_0 = l_1 \sin\vartheta_1 \tag{2}$$

$$\beta = \tan^{-1}\left(\frac{h_x + h_0 + l_1 \sin\vartheta_1 + l_2 \sin\vartheta_2 - h_{x1}\cos\vartheta_2}{l_1 \cos\vartheta_1 + l_2 \cos\vartheta_2 + h_{x1}\sin\vartheta_2}\right) \tag{3}$$

The stroke of the actuator C_{Att} depends on the length of the tendon l_5 and the preload stroke of the spring, C_{Att1}, and is calculated by solving Eq. (4):

$$C_{Att} = l_{5\max} - l_5 + C_{Att1}, \qquad l_5 = \frac{l_4 \cos\alpha_1 + (h_2 + h_{x1})\sin\vartheta_2}{\cos\beta} \tag{4}$$

The value of $l_{5\max}$ corresponds to the maximum length XX_1 of the tendon (Figure 3b), that is at the maximum flexion of the finger. The trajectory of the fingertip in the (u,w) plane (Figure 3a) is then calculated.

The force F applied to the fingertip is evaluated for each value of α_1 considering the equilibrium of link 2 (Figure 5). The direction of F is considered as perpendicular to the link 2 in point P due to sliding between the fingertip and the support. The equivalent mass of the system m_c has been considered as centered at point G belonging to the link 2. The static analysis yields the following Eq. (5-7):

$$-F_B \cdot \cos\vartheta_1 + F_A \cdot \cos\alpha_1 - F_x \cdot \cos\beta = F \cdot \sin\vartheta_2 \tag{5}$$

$$F_B \cdot \sin\vartheta_1 - F_A \cdot \sin\alpha_1 + F_x \cdot \sin\beta = F \cdot \cos\vartheta_2 + m_c \cdot g \tag{6}$$

$$\begin{aligned} &F_A \cdot \left[\cos\alpha_1 \cdot (l_2 \cdot \sin\vartheta_2 + h_2 \cdot \cos\vartheta_2) - \sin\alpha_1 \cdot (l_2 \cdot \cos\vartheta_2 + h_2 \cdot \sin\vartheta_2)\right] \\ &+F_x \cdot \left[\cos\beta \cdot (h_{x1} \cdot \cos\vartheta_2 - l_2 \cdot \sin\vartheta_2) + \sin\beta \cdot (h_{x1} \cdot \sin\vartheta_2 + l_2 \cdot \cos\vartheta_2\right] \\ &= F \cdot (l_2 + d_2) + m_c \cdot g \cdot \cos\vartheta_2 \cdot (g_2 + l_2) \end{aligned} \tag{7}$$

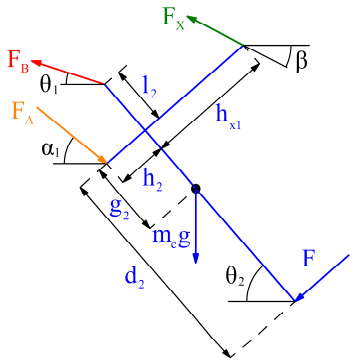

Fig. 5. The free body diagram of the coupler of the linkage.

Given the feedback force F, it is possible to calculate the force error e, being the force reference F_{ref} a function of the position of the fingertip, i.e. of the rocker α_1:

$$e = F_{ref} - F \qquad F_{ref} = F_{ref}(\alpha_1) \tag{8}$$

Due to its simplicity, a proportional-integral-derivative (PID) controller has been used:

$$V_{ref} = K_P e + K_I \int_0^t e dt + K_D \frac{de}{dt} \tag{9}$$

where K_P, K_I and K_D are, respectively, the proportional, integral and derivative gains. An iterative approach has been used for the definition of the control logic parameters: finally, a simple proportional control came out to be sufficiently accurate and stable for the application.

A second order system transfer function has been used to simulate the dynamic behavior of the pressure control proportional valve (*Pressure Control Valve* block):

$$p_1 = \frac{K_V \sigma_n^{\,2}}{s^2 + 2\zeta\sigma_n s + \sigma_n^{\,2}} V_{ref} \tag{10}$$

where K_V is the static gain, σ_n the natural frequency and ζ the damping factor of the valve.

The pneumatic resistance (*Fluidic Resistance* block) has been modeled according to the ISO 6358 [9]. The mass air flow passing through the resistance can be

calculated in sonic or subsonic condition depending on the ratio between the downstream and upstream pressures, as presented in Eq. (4):

$$G = \rho_0 P_1 C \ for\ 0 < \frac{P_{mu}}{P_1} \le b, \quad G = \rho_0 P_1 C \sqrt{1 - \left(\frac{P_{mu}/P_1 - b}{1-b} \right)^2} \ for\ b < \frac{P_{mu}}{P_1} \le 1 \tag{11}$$

where P_1 is the upstream absolute pressure, P_{mu} is the downstream absolute pressure, C is the sonic conductance, b is the critical ratio and ρ_0=1.18 kg/m^3 is the air density in normal conditions. The C and b parameters are reported in Table 1.

Being R=287.2 J/(kgK) the air constant, T the absolute air temperature, assuming the variation of the internal volume V of the pneumatic muscle as negligible, the time derivative of the absolute internal pressure of the muscle for an isothermal transformation can be expressed as:

$$\frac{dP_{mu}}{dt} = \frac{RT}{V} G = \frac{RT}{\pi r^2 l} G \tag{12}$$

with the actual l length and the radius r of the actuator given by [d]:

$$l = l_0 - C_{Att}, \quad r = \frac{\sqrt{h^2 - l^2}}{2\pi n_t} \tag{13}$$

where C_{att} is the stroke of the pneumatic muscle whose initial pre-loaded length is l_0, n_t is the number of turns of the fibers, whose length h is 178 mm for the employed McKibben muscle with 20 mm diameter.

The internal relative pressure of the muscle p_{mu} can be calculated integrating Eq. (12). Therefore, the force exerted by the muscle is given by Eq. (14) as a function of the internal pressure of the actuator [10]:

$$F_{mu} = -p_{mu} \frac{h^2 - l^2}{4\pi n_t^2} + E \frac{l - l_i}{l_i} 2 r_i \pi s_i + \left[p_{mu} l \frac{\sqrt{h^2 - l^2}}{2\pi n_t} - \frac{E s_i l}{r_i} \left(\frac{\sqrt{h^2 - l^2}}{2\pi n_t} - r_i \right) \right] \frac{l}{n_t \sqrt{h^2 - l^2}} \tag{14}$$

where r_i and l_i are respectively the initial radius and length of the muscle at rest, s_i is the initial thickness of the inner chamber, E is the Young modulus of the chamber.

Finally, the force F_x is directly connected to the force exerted by the muscle F_{mu} and the spring F_m by the following relations:

$$F_x = F_{mu} - F_m, \qquad F_m = k_m \cdot C_{Att} + F_{m0} \tag{15}$$

where k_m is the spring constant, and F_{m0} its preload.

Table 1. Parameters of the model.

Parameter	Value		Parameter	Value		Parameter	Value	
l_1	55	mm	h_{x1}	18	mm	n_t	1,52	
l_2	5	mm	k_m	140	N/m	E	0.95	MPa
d_2	25	mm	F_{m0}	13.934	N	K_P	0.28	V/N
g_2	13	mm	C_{Att1}	20	mm	K_V	1e5	Pa/V
h_2	7	mm	m_c	55	g	ζ	1.8	
l_4	63.9	mm	l_0	162	mm	σ_n	140	rad/s
l_{5max}	81.4	mm	l_i	110	mm	C	5.25e-9	$m^3Pa^{-1}s^{-1}$
h_0	15	mm	r_i	10	mm	b	0.39	
h_x	0	mm	s_i	0.8	mm	K_{obj}	8	N/rad

4. Simulation and experimental validation

In order to evaluate the ability of the device to generate a haptic feedback in dynamic condition, corresponding to the interaction between the remote unit and the environment (whether a real or virtual one), some experimental tests were carried out on the prototype. The outcomes of the trials have been also used to validate the model described in the previous paragraph.

The results presented in Figure 6 refer to the case in which the operator, freely moving his finger, handles a virtual object whose crushing force is proportional to the rotation of rocker α_1, i.e. to the reference feedback force $F_{ref}=K_{obj}\,\Delta\alpha_1$, with the stiffness constant K_{obj} set to 8 N/rad. Figure 6a shows the force signal acquired experimentally, compared to the one provided by the simulation, and obtained considering the same rotation pattern $\alpha_1(t)$. This comparison highlights the ability of the model to predict the trend of the force generated by the device in dynamic condition with good precision. The Figure 6b shows the relationship between the force generated on the fingertip F and the rotation angle α_1 of the rocker, in both experimental and simulated conditions.

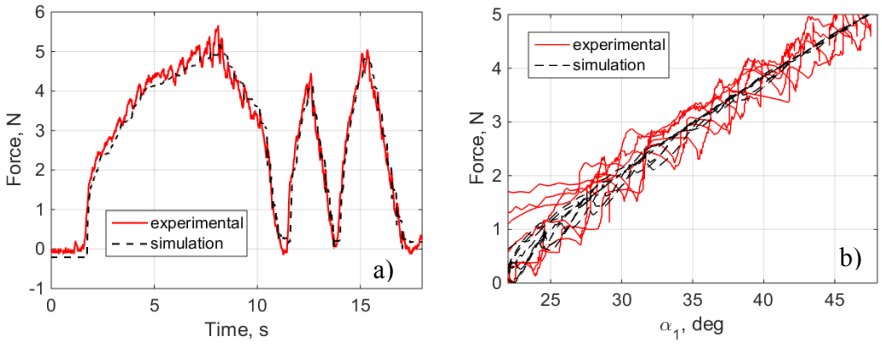

Fig. 6. Comparison between experimental and simulation results (K_{ogg} = 8 N/rad).

The relationship between the force F and the angle of rotation α_1 of the rocker depends on the mechanical characteristics of the virtual object and it is influenced by the performance of the system. In fact, any oscillation in the contact force F affects negatively the ability of the device to provide the correct haptic feedback to the operator. Probably they are due to the behavior of the control logic and eased by the elasticity of both the mechanism and the actuation group. The entity of such oscillations could be relevant for some applications. To overcome this issue, a different design of the control logic and the use of a dumper may be necessary.

5. Conclusion

This work demonstrated that the proposed haptic system, based on a four-bar mechanism, and actuated by a McKibben pneumatic artificial muscle, is able to generate the required perception force at the operator's fingertip, with good performance both in static and dynamic conditions. Therefore, it could be used as a base for the development of hand haptic exoskeletons. In addition, the proposed model proved to be able to predict with good accuracy the behavior of the system, and may be used for the design and optimization of such devices.

References

1. D. Maffiodo and T. Raparelli, “Three-Fingered Gripper with Flexure Hinges Actuated by Shape Memory Alloy Wires”, International Journal of Automation Technology, vol. 11, no. 3, pp. 355-360, 2017.
2. C. Ferraresi, W. Franco and G. Quaglia, “A novel bi-directional deformable fluid actuator”, Proceedings of the Institution of Mechanical Engineers, Part C: Journal of Mechanical Engineering Science, vol. 228, no. 15, pp. 2799-2809, 2014.
3. Z. Sun, G. Bao, Q. Yang and Z. Wang, “Design of a Novel Force Feedback Dataglove Based on Pneumatic Artificial Muscles”, 2006 International Conference on Mechatronics and Automation, Luoyang, Henan, pp. 968-972, 2006.
4. H. Li, K. Kawashima, K. Todano, S. Ganguly and S. Nakano, “Achieving Haptic Perception in Forceps’ Manipulator Using Pneumatic Artificial Muscle”, IEEE/ASME Transactions on Mechatronics, vol.18, no. 1, February 2013pp.74-85.
5. K. MooD. Ryu, C. Chun, Y. Lee, S. Kang, M. Park, “Development of a Slim Haptic Glove Using McKibben Artificial Muscles”, SICE-ICASE International Joint Conference, Bexco, Busan, Korea, Oct. 18-21, 2006, pp. 204-208.
6. M. Egawa, T. Watanabe and T. Nakamura, “Development of a Wearable Haptic Device with Pneumatic Artificial Muscles and MR brake”, IEEE Virtual Reality (VR), Arles, pp. 173-174, 2015.
7. C. Ferraresi, W. Franco, A. Manuello Bertetto and F. Pescarmona, “Study of a haptic finger actuated by pneumatic muscles”, 7th Int Symp on Fluid Control, Measurement and Visualization Flucome 2003, Sorrento, pp. 6, 2003.
8. C. De Benedictis, C. Ferraresi, W. Franco, D. Maffiodo, “Hand rehabilitation device actuated by a pneumatic muscle”, 27th International Conference on Robotics in Alpe-Adria-Danube Region, RAAD 2018, Patras, Greece, 6-8 June, 2018.
9. C. Ferraresi, “Modelling of pneumatic systems”, Fluid Apparecchiature Idrauliche & Pneumatiche, vol. 346, pp. 48–54, 1993.
10. C. Ferraresi, W. Franco and A. Manuello Bertetto, “Flexible Pneumatic Actuators: a comparison between the McKibben and the straight fibres muscle”, Journal of Robotics and Mechatronics, vol. 13, no. 1, pp. 56-63, 2001.